RESEARCH PAPER

The effects of nano-chitosan loaded with gallic acid as an antibacterial and remineralizing agent on some properties of orthodontic adhesive

Lara Riyadh Al-Banaa[1*], Ali R. Al-Khatib[1], Fawzi Habeeb Jabrail[2]

[1] Department of Pedodontics, Orthodontic and Preventive Dentistry, College of Dentistry, Mosul University, Iraq
[2] Department of Chemistry, College of Science, University of Mosul, Mosul, Iraq

ABSTRACT

Objective(s): This study aimed to evaluate the effect of adding nano-chitosan loaded with gallic acid to an orthodontic primer as an antimicrobial and remineralizing agent while preserving orthodontic adhesive's physical and chemical properties.

Materials and methods: Nano-chitosan loaded with gallic acid was added to Transbond XT primer to form nano-chitosan/gallic acid primer. This study compared three groups: control without additive, 5%, and 10% Nano-Chitosan/Gallic acid Primer (NCGP). In terms of FTIR, Shear Bond Strength (SBS), Adhesive Remnant Index (ARI), Degree of monomer Conversion (DC), antibacterial properties against *Streptococcus mutans* and *Lactobacillus acidophilus*, and Field Emission Scanning Electron Microscopy with Energy Dispersive X-ray spectroscopy (FESEM-EDX) were examined to detect remineralization of demineralized enamel.

Results: Both the 5% and 10% nano-chitosan/gallic acid primer groups demonstrated significant antibacterial activity, a 15–20% increase in shear bond strength (SBS), a 10–15% enhancement in the degree of monomer conversion (DC), and a 30–40% increase in calcium and phosphate weight percentages compared to the control group. Additionally, no significant differences were observed in Adhesive remnant index (ARI) scores among the groups.

Conclusions: The orthodontic adhesive primer modified with nano-chitosan loaded with gallic acid demonstrated enhanced mechanical, chemical, antibacterial, and remineralizing properties compared to the commercial adhesive. Therefore, it can be considered a novel adhesive for treating white spot lesions (WSLs).

Keywords: *Chitosan, FESEM, Nanoparticles, Shear bond strength, White spot lesions*

How to cite this article

Al-Banaa LR, Al-Khatib AR, Jabrail FH. The effects of nano-chitosan loaded with gallic acid as an antibacterial and remineralizing agent on some properties of orthodontic adhesive. Nanomed J. 2025; 12: 1-. DOI: 10.22038/NMJ.2025.81400.2023

INTRODUCTION

White-spot lesions (WSLs) are common side effects of fixed orthodontic treatment, characterized by enamel demineralization that appears as chalky white, non-cavitated areas. These early stages of dental caries result from bacterial plaque activity and retain the potential for remineralization [1,2]. Fixed orthodontic appliances increase the risk of developing WSLs due to the irregular surfaces of wires, bands, and brackets, impairing saliva's normal cleansing function, leading to food and plaque accumulation. This accumulation can be colonized by acid-producing bacteria such as *Streptococcus mutans* and *Lactobacillus* species. Furthermore, etching the enamel with phosphoric acid before bracket bonding with composite resins causes superficial demineralization. WSLs have been reported in up to 97% of patients following fixed appliance therapy [3,4].

Various approaches, including improved oral hygiene, low-carbohydrate diets, and topical fluoride treatments, have been investigated to reduce the incidence of WSLs. However, these methods are often unreliable because they depend on patient compliance. Therefore, preventive strategies not relying on patient cooperation may

*Corresponding author(s) Email: dr-lara-ra@uomosul.edu.iq
Note. This manuscript was submitted on July 27, 2024; approved on March 03, 2025.

be more effective in reducing WSLs [5]. One promising approach to prevent enamel demineralization involves using novel orthodontic bonding materials with inherent antibacterial and remineralization properties [6,7]. Previous studies have focused on enhancing orthodontic adhesives by incorporating new antibacterial agents such as titanium oxide, nano-silver, quaternary ammonium compounds, and chlorhexidine [8,9].

Furthermore, various remineralization agents have demonstrated successful treatment of WSLs, including fluoride, calcium carbonate ($CaCO_3$), casein phosphopeptide (CPP), amorphous calcium phosphate (ACP), hydroxyapatite (HAP), and others [10].

Gallic acid, a natural compound extracted from various plants such as oak bark, tea leaves, and Galla chinensis extract, possesses a chemical structure of 3,4,5-trihydroxybenzoic acid. It has been confirmed as a potent antibacterial agent and can influence the demineralization and remineralization of dental hard tissues by interacting with structural proteins and calcium. Polarized light microscopy has demonstrated that gallic acid can reduce the depth of carious lesions in in vitro studies [11,12].

Chitosan is a natural carbohydrate polymer produced by the de-N-acetylation of chitin, the main component of crustacean exoskeletons. It has been approved by the Food and Drug Administration (FDA) as a food ingredient due to its biocompatibility, non-toxicity, and biodegradability [13]. Additionally, chitosan exhibits antibacterial properties by causing the displacement of Ca^{2+} ions from anionic sites in the bacterial cell wall membrane, leading to cell death [14].

Chitosan is a natural remineralizing agent with many applications in restorative and orthodontic research for remineralizing enamel and dentin [15]. When combined with other bioactive materials, the active sites within the chitosan structure function as a drug delivery system, serving as an ion reservoir essential for remineralization. Furthermore, these materials immobilize hydroxyapatite nano-building units and provide a scaffold for their structural organization [16,17]. Chitosan nanoparticles possess a larger surface area and higher reactivity, allowing for the slow and controlled release of active agents required for long-term orthodontic treatment [18].

In this study, chitosan nanoparticles were loaded with gallic acid to produce a synergistic effect for antibacterial activity and remineralization of demineralized enamel.

Previous analyses have shown that no study has investigated the remineralization and antibacterial properties of adding nano-chitosan loaded with gallic acid to an orthodontic primer. The null hypothesis of this study was that adding nano-chitosan loaded with gallic acid to the primer (NCGP) does not affect the orthodontic adhesive's remineralization, antibacterial, physical, or chemical properties.

This study examines the effect of adding nano-chitosan loaded with gallic acid to the orthodontic primer (NCGP) as an antimicrobial and remineralizing agent, while maintaining the orthodontic adhesive's acceptable physical and chemical properties.

MATERIAL AND METHODS

This research was approved by the ethical committee at the College of Dentistry/University of Mosul under the number (UoM.Dent. 23/24) on 02/5/2023.

Gallic acid (3,4,5-trihydroxybenzoic acid) was purchased from Sigma-Aldrich (Germany) with a molecular weight of 170.12 and linear formula (HO)3C6H2CO2H.

Nano-chitosan powder was purchased from Nanochemazone Company (Canada), with the molecular formula $C_6H_{11}NO_4$, a purity of 99.9%, and a molecular weight of 161 g/mol. Nano-chitosan was characterized by FESEM-EDX (TESCAN, MIRA3, France) operated at 20 kV and 10 mA. A small amount of the powder was spread onto adhesive carbon tapes and coated with a thin layer of gold (10 nm).

The FESEM images showed particles within the nanoscale range (30–50 nm), with spherical or semi-oval shapes. The EDX analysis revealed a higher proportion of carbon (C) and oxygen (O) with a smaller percentage of nitrogen (N) (Fig. 1).

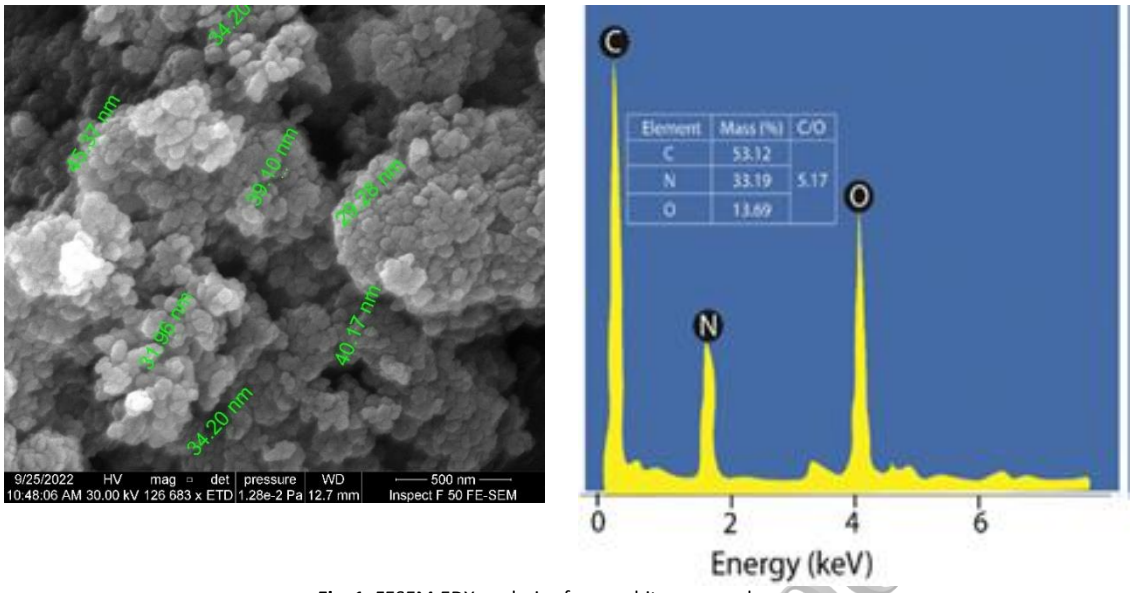

Fig. 1. FESEM-EDX analysis of nano-chitosan powder

Preparation of Nano-Chitosan loaded with gallic acid hydrogel

The chitosan solution was prepared by dissolving 1.0 g of nano-chitosan powder in 100 mL of deionized distilled water. Then, 1 mL of 2% (v/v) acetic acid solution (Merck KGaA, Darmstadt, Germany) was added dropwise to the chitosan solution and mixed under magnetic stirring for approximately 3 hours to produce a homogeneous nano-chitosan solution. The pH of the solution was adjusted to 7.0 by the dropwise addition of 0.05 mol NaOH solution [19].

The nano-chitosan loaded with gallic acid hydrogel was prepared by mixing nano-chitosan and gallic acid at a weight ratio of 5:1. Specifically, 200 mg of gallic acid powder was added to the dissolved chitosan solution and stirred magnetically for 1 hour at room temperature [20].

Preparation of the modified orthodontic primer

Transbond XT primer (3M Unitek, Monrovia, USA), the gold standard orthodontic adhesive, was used to prepare nano-chitosan-loaded gallic acid primers (NCGP) at 0%, 5%, and 10% weight-to-weight ratios. According to the method described by Nader et al. [13], one drop of primer (50 µL in volume) was drawn using a micropipette (10–100 µL range) for standardization. A digital scale with 0.001 mg accuracy was used to weigh one drop, which was approximately 0.05 g. Twenty drops of modified primer were prepared for each group by mixing 1 g of primer with 0.05 g and 0.1 g of nano-chitosan/gallic acid to produce the 5% and 10% NCGP groups, respectively, in addition to a control group without additives. Mixing was performed in a semi-dark environment inside microtubes using the straight head of a dental probe until a uniform consistency was achieved. Furthermore, an ultrasonic bath was applied for 30 minutes to ensure better material dispersion within the primer. The microtubes were wrapped with dark tape to prevent light exposure.

Testing procedures

1. *Characterization of nano-chitosan/gallic acid hydrogel by FESEM-EDX*

FESEM was used to evaluate the morphology and distribution of gallic acid particles within the nano-chitosan hydrogel. EDX analysis was performed to determine the elemental composition of the prepared material.

2. Fourier Transform Infrared Spectrometry (FTIR) of modified primer

The chemical properties of the primer before and after modification with nano-chitosan-gallic acid hydrogel were analyzed using Fourier Transform Infrared Spectroscopy (FTIR/ATR Alpha II, Platinum, Bruker Optics, Germany) over the wavelength range of 400–4000 cm^{-1}. The FTIR spectrum of the unmodified primer was used as a reference to identify the changes detected [21].

3. Degree of Monomer Conversion (DC)

The degree of conversion (DC) was assessed using FTIR spectroscopy [22,23]. Sample preparation (n = 5 per group) involved applying a drop of primer onto a celluloid strip fixed over a

glass slide, which was then lightly pressed by another strip and light-cured at 1500 W/cm² for 10 seconds (5 seconds from each side). A standard distance of 1 mm was maintained between the tip of the light-curing unit and the sample. The upper celluloid strips were then removed, and the cured specimen, approximately 0.1 mm thick and measuring 4 × 4 mm, was carefully excised with a narrow surgical blade and stored in a dark, dry container for 24 hours until analysis. The specimen was placed on the diamond ATR crystal of the FTIR spectrometer equipped with attenuated total reflection (ATR). The spectrum was acquired in absorbance mode over a wavelength range of 400–4000 cm^{-1}, with 24 scans at a resolution of 4 cm^{-1}. Non-cured drops of control and modified primer specimens were also subjected to FTIR analysis. The DC% was calculated using a relative percentage method (tangent baseline and two-frequency method) by comparing the C═C aliphatic bond stretching vibrations (analytical peak at 1638 cm^{-1}) with the C=C aromatic bond stretching vibrations (reference peak at 1608 cm^{-1}), which remain unaffected by the polymerization reaction. The following equation was used to determine the DC:

Where A (C=C), A(C..C) present the net peak absorbance areas of the set (P) and unset (M) material at the specific bands, respectively.

4. Shear bond strength (SBS)

This study utilized 30 extracted upper first premolar teeth obtained for orthodontic reasons, ensuring they were free from caries, restorations, and enamel cracks. The teeth were stored in a 0.1% thymol solution to prevent bacterial growth [24] and then mounted in plastic rings up to the cementoenamel junction using cold-cure acrylic resin.

Three groups of teeth (n = 10 each) were randomly selected and divided into: control group, 5% NCGP, and 10% NCGP. After polishing the buccal surfaces with non-fluoridated pumice, the teeth were rinsed with water and dried. For bracket bonding, the teeth were etched with 37% phosphoric acid for 20 seconds, rinsed for 10 seconds, and air-dried. Both unmodified and modified primers were applied to the premolar buccal surfaces, followed by gentle airflow to disperse excess primer. Orthodontic brackets (stainless steel metallic brackets, standard edgewise type, Dentaurum, Germany) were positioned using a Boone gauge approximately 4 mm from the tip of the buccal cusp [25] and pressed with a 200 g load. After removing excess adhesive, the brackets were light-cured for 40 seconds using an LED curing device (1500 mW/cm²). Shear bond strength (SBS) was measured using a universal testing machine (Gester Instrument Co., Fujian, PR China) by positioning a knife-edge chisel at the tooth-bracket interface, directed in an occlusal-gingival direction (Fig. 2). The crosshead speed was set at 0.5 mm/min. The fracture force results were electronically recorded in Newtons and converted to megapascals by dividing the force by the surface area of the bracket base [26].

Fig. 2. Loading of the bracket under shear force in SBS testing setup

5. Adhesive remnant index (ARI)

The ARI was assessed by inspecting the residual adhesive on both the tooth and bracket base after measuring the SBS of debonded brackets under 10x magnification with a stereomicroscope. The ARI scores are as follows [27, 28]:

Score 0: No remaining adhesive on the enamel surface.

Score 1: Less than half of the remaining adhesive is on the enamel surface.

Score 2: Over half of the remaining adhesive is on the enamel surface.

Score 3: All the adhesive remained on the enamel surface with a clear impression of the bracket's mesh.

6. Antibacterial assessment: Disc diffusion method (Kirby-Bauer method)

The antibacterial properties of the modified adhesive primer discs were tested against two cariogenic bacteria: Streptococcus mutans (Gram-positive cocci) and Lactobacillus acidophilus (Gram-

positive bacilli). Plastic molds (6 mm diameter and 2 mm thickness) were used to fabricate discs for the control, 5% NCGP, and 10% NCGP groups (total discs = 15; n = 5 per group). The primer was poured into the molds and light-cured for 10 seconds on the top and 10 seconds on the bottom. After curing, the discs were removed from the molds and sterilized with 70% ethanol for 30 minutes at room temperature.

About 20 mL of Mueller–Hinton powder was dissolved in 1 L of distilled water to prepare the agar plates, which were then cooled to 45–50°C. The mixture was poured into sterilized Petri dishes to a thickness of 4 mm. The agar was allowed to solidify at room temperature and then stored at 4°C until use. Brain heart infusion (BHI) broth was used to individually culture Streptococcus mutans [29] and Lactobacillus species. After adjusting the turbidity to 0.5 McFarland standard (approximately 1.5×10^8 cells/mL), the tubes were incubated for 24 hours at 37°C.

A sterile wire loop was used to smear the bacterial culture onto Mueller–Hinton agar plates, and the agar surface was allowed to dry for approximately 5 minutes. The discs were gently pressed onto the agar using sterilized forceps. Plates were incubated under anaerobic conditions at 37°C for 24 hours. The bacterial inhibition zones around the discs were measured in millimeters. Five Petri dishes were used for each bacterial species, containing three discs: control, 5% NCGP, and 10% NCGP [27].

7. FESEM-EDX Analysis of remineralization

Fifteen crown surfaces of upper premolars from all groups (n = 5 each) were subjected to demineralization to prevent false-positive remineralization results. First, the crowns were coated with an acid-resistant varnish, exposing an enamel window of approximately 3 × 4 mm at the middle third of the buccal surface. In contrast, the varnish protected the rest of the crown. Each group was immersed in 40 mL of acidified buffered demineralizing solution at room temperature for 96 hours to induce initial artificial carious lesions. The demineralizing solution contained 2.2 mmol/L $CaCl_2$, 2.2 mmol/L NaH_2PO_4, and 50 mmol/L acetic acid, with the pH adjusted to 4.5 using NaOH [30]. After removal from the solution, the specimens were washed and dried. The exposed enamel windows of the demineralized specimens were etched and bonded with either the control primer, 5% NCGP, or 10% NCGP. Each group was stored in containers containing 40 mL of artificial saliva for 4 months. The artificial saliva composition was as follows [31]: 0.4 g/L KCl, 0.4 g/L NaCl, 0.795 g/L $CaCl_2 \cdot 2H_2O$, 0.780 g/L $NaH_2PO_4 \cdot 2H_2O$, 0.005 g/L $Na_2S \cdot 9H_2O$, and 1 g/L urea, all dissolved in 1000 mL of distilled water.

For SEM-EDX analysis, the crowns were separated from the roots, and a longitudinal section in the buccolingual direction at the mid-occlusal surface of the premolars was performed using a water-cooled, low-speed handpiece with double sided diamond disc. The cut surfaces were stored in distilled water until further analysis.

All specimens were thoroughly dehydrated and then coated with a thin layer of gold to prepare the surface for field emission scanning electron microscopy (FESEM) examination.

Elemental analysis (calcium and phosphate weight percentages) was performed using the EDX unit attached to the same FESEM instrument. The cut surfaces were carefully examined at a depth of 100 µm from the bonding surface to obtain representative photomicrographs and quantitative measurements.

Statistical analysis

Statistical analysis was performed using SPSS software version 26. The study results were analyzed by one-way analysis of variance (ANOVA) followed by the post-hoc Tukey test. Adhesive Remnant Index (ARI) scores were compared using the Chi-square test. Statistical significance was set at $p < 0.05$.

RESULTS

1. Characterization of nano-chitosan/gallic acid by FESEM-EDX

FESEM images of the prepared chitosan/gallic acid hydrogel (Fig. 3A) showed a homogeneous morphology of the chitosan matrix. The gallic acid particles appeared as white spots at the nanoscale (20–40 nm) and were uniformly distributed throughout the chitosan matrix.

The EDX analysis of the chitosan/gallic acid hydrogel revealed a higher proportion of carbon (C) and oxygen (O), with a smaller percentage of nitrogen (N) (Fig. 3B).

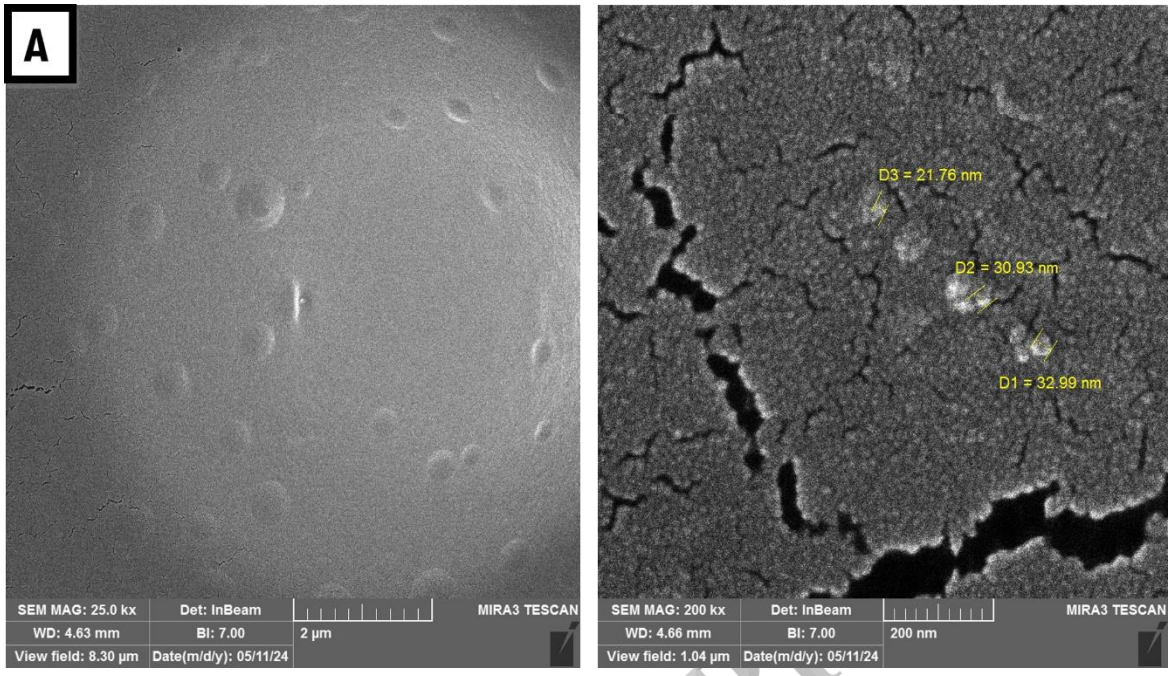

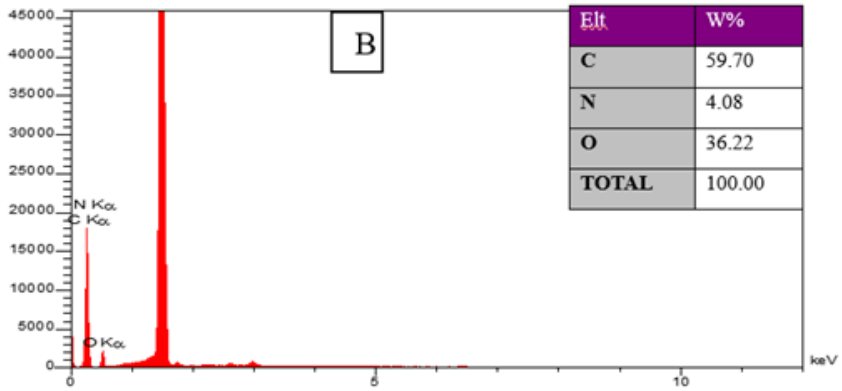

Elt	W%
C	59.70
N	4.08
O	36.22
TOTAL	100.00

Fig 3. (A) FESEM image of Nano-Chitosan/ Gallic acid hydrogel at 25 and 200 kx magnification showing gallic acid particle sizes, shapes and distribution within the chitosan matrix; (B) EDX spectrum with elements percentage in weight of the prepared hydrogel

2. FTIR Characterization of modified primer by Nano-Chitosan /Gallic acid

Figures 4A, 4B, and 4C show the FTIR spectra of all groups, with no appearance or disappearance of bands, indicating that no chemical reaction occurred between the primer and the chitosan loaded with gallic acid at 5% and 10%.

Chitosan/gallic acid exhibits a distinct peak at 3482 cm^{-1} corresponding to the hydroxyl stretch (O–H). Chitosan also peaks at 1636 cm^{-1} attributed to the C=O stretch of the amide I band. Gallic acid presents peaks at 1714 cm^{-1} and 1453 cm^{-1} due to C=O and C–H stretching, respectively.

The FTIR spectrum of the primer displays characteristic peaks at 3482 cm^{-1}, 2959 cm^{-1}, 1714 cm^{-1}, and 1636 cm^{-1}, corresponding to hydroxyl (O–H), aliphatic (C–H), carbonyl (C=O), and alkene (C=C) stretching vibrations, respectively. These peaks overlap with those of chitosan/gallic acid, resulting in no additional peaks observed between the FTIR spectra of the unmodified and modified primers.

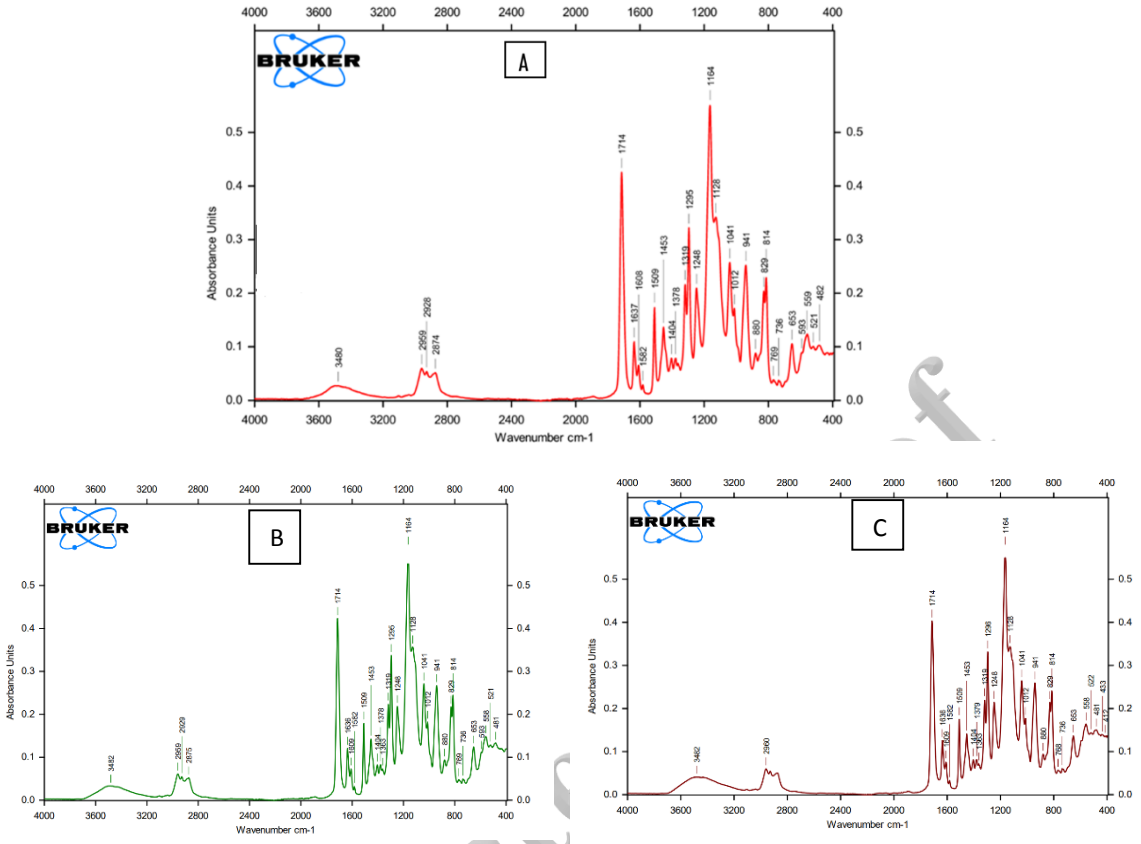

Fig. 4. FTIR spectra of (A) control; (B) 5% NCGP; (C) 10% NCGP

Table 1. Descriptive statistics and multiple comparisons Post-hoc Tukey test of shear bond strength and Degree of Conversion of the control, 5% NCGP, 10% NCGP

	shear bond strength							Degree of Conversion						
Groups	**N**	**Mean**	**SD**	**Min.**	**Max.**	**p – value**	**Post-hoc test***	**n**	**Mean**	**SD**	**Min.**	**Max.**	**p - value**	**Post-hoc test***
Control	10	15.20	.60	11.80	18.20	0.04	A	5	60.26	1.25	58.50	62.00	0.000	A
5% NCGP	10	17.28	1.07	12.50	24.10		A,B	5	66.21	.55	65.50	67.00		B
10% NCGP	10	18.27	.70	14.70	21.10		B	5	69.00	1.96	66.70	72.00		C

NCGP: Nano-Chitosan/Gallic acid Primer, SD: Standard deviation, Different litters mean significant difference at (P ≤ 0.05).

3. Degree of Conversion

Table 1 shows that the highest significant mean degree of conversion (DC) was observed in the 10% NCGP group (69%), followed by the 5% NCGP group (66.2%). The control group exhibited the significantly lowest DC value (60.2%).

4. Shear bond strength

The 10% NCGP group exhibited the highest mean shear bond strength (SBS) of 18.27 MPa (Table 1), followed by the 5% NCGP group with 17.28 MPa, while the control group had the lowest mean value at 15.20 MPa. SBS increased significantly in the 10% NCGP group compared to the unmodified control group. The 5% NCGP group showed no significant difference in SBS compared to the control and 10% NCGP groups.

5. Adhesive remnant index

The ARI bar chart (Fig. 5, Table 2) showed no significant differences among the three groups, with the majority of specimens (16) scoring 3, indicating that the adhesive remained on the enamel after bracket debonding. Eleven specimens scored 2, while the remaining three specimens scored 1.

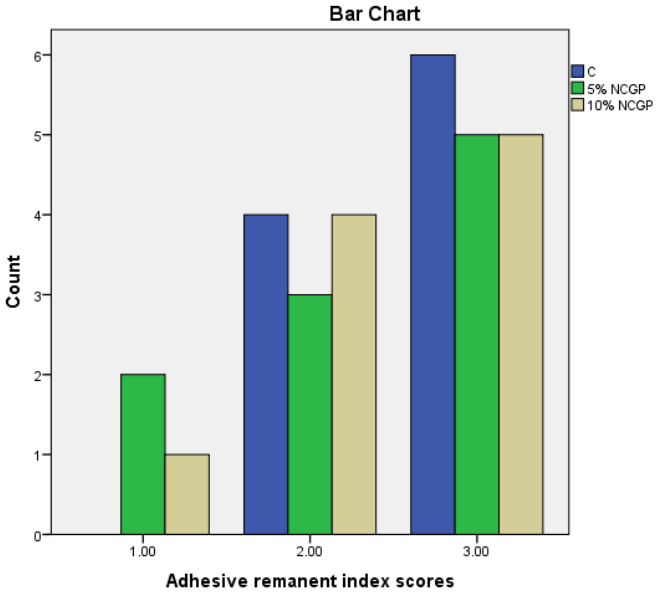

Fig. 5. Bar chart representing the ARI scores: C is control group, NCGP is Nano-Chitosan/Gallic acid Primer

Table 2. Frequency and percentage of adhesive remnant index (ARI) scores.

Groups	ARI SCORES				Total
	0	1	2	3	
Control (N=10)	0	0	4	6	10
NCGP 5% (N=10)	0	2	3	5	10
NCGP10%	0	1	4	5	10
Total	0(0%)	3(10%)	11(36.66%)	16(53.33%)	30

NCGP: Nano-Chitosan/Gallic acid Primer.

6. Antibacterial activity

The results of the antimicrobial test showed that experimental discs containing both 5% and 10% NCGP exhibited antibacterial activity against *Streptococcus mutans* and *Lactobacillus acidophilus*, demonstrated by the presence of clear inhibition zones around the discs on the agar plates, as shown in Figures 6A and 6B. The control group showed no antibacterial effect (no clear zone around the disc). The antibacterial activity increased significantly from 5% to 10% NCGP (Table 3).

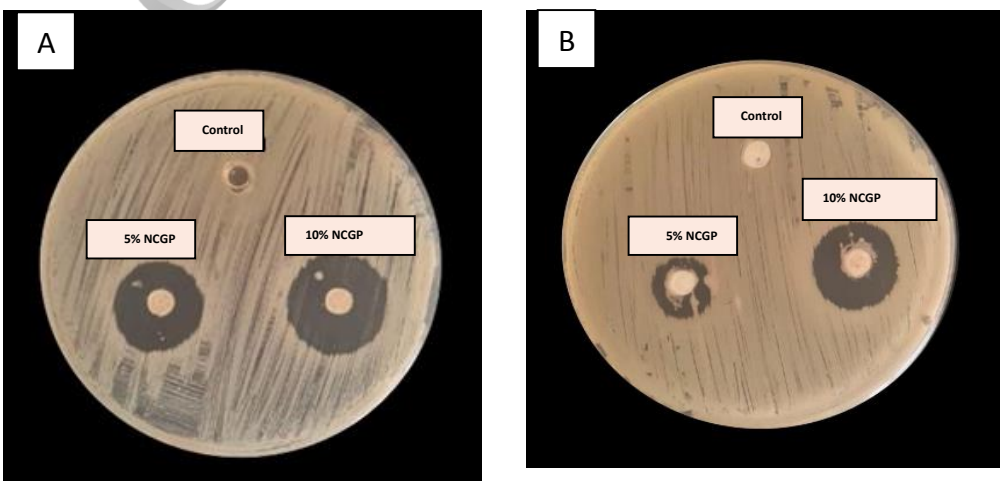

Fig. 6. Bacterial inhibition zone of control group, 5% and 10% Nano-Chitosan/Gallic acid Primer groups against: (A) *Streptococcus mutans* and (B) *Lactobacillus acidophilus.*

Table 3. Descriptive statistics and multiple comparisons Post-hoc Tukey test of *streptococcus mutans* and *lactobacillius* growth inhibition of the control, 5% NCGP, 10% NCGP.

	Streptococcus mutans							Lactobacillus acidophilus						
Groups	**n**	**Mean**	**SD**	**Min.**	**Max.**	**p - value**	**Post-hoc test***	**n**	**Mean**	**SD**	**Min.**	**Max.**	**p - value**	**Post-hoc test***
Control	5	.00	.00	.00	.00		A	5	.00	.00	.00	.00		A
5% NCGP	5	14.62	1.00	13.70	15.90	0.000	B	5	10.94	.75	10.00	12.00	0.000	B
10% NCGP	5	16.90	.53	16.00	17.30		C	5	16.58	.74	15.70	17.60		C

NCGP: Nano-Chitosan/Gallic acid Primer, SD: Standard deviation, Different litters mean significant difference (P ≤ 0.05).

7. FESEM-EDX analysis of remineralization

The FESEM images in Figure 7 (A1 to C3) revealed the morphology, crystalline phases, and mineral deposition on the surfaces of both the treated and untreated groups.

The morphology of the enamel surfaces of specimens treated with chitosan loaded with gallic acid primer after remineralization showed noticeable changes in the enamel rod nanostructure and a reduction in the inter-rod spaces. Newly formed grain-like materials (~50 nm) enhanced the nanocrystalline enamel structure, including the prism and inter-prismatic zones. Upon completion of remineralization, enamel-like structures covered the entire demineralized lesion. These newly formed structures result from non-classical crystallization processes. Moreover, the 10% NCGP group exhibited mineral deposition and formation of hydroxyapatite layers on the demineralized enamel, which were absent in the control group (Fig. 7C2, C3).

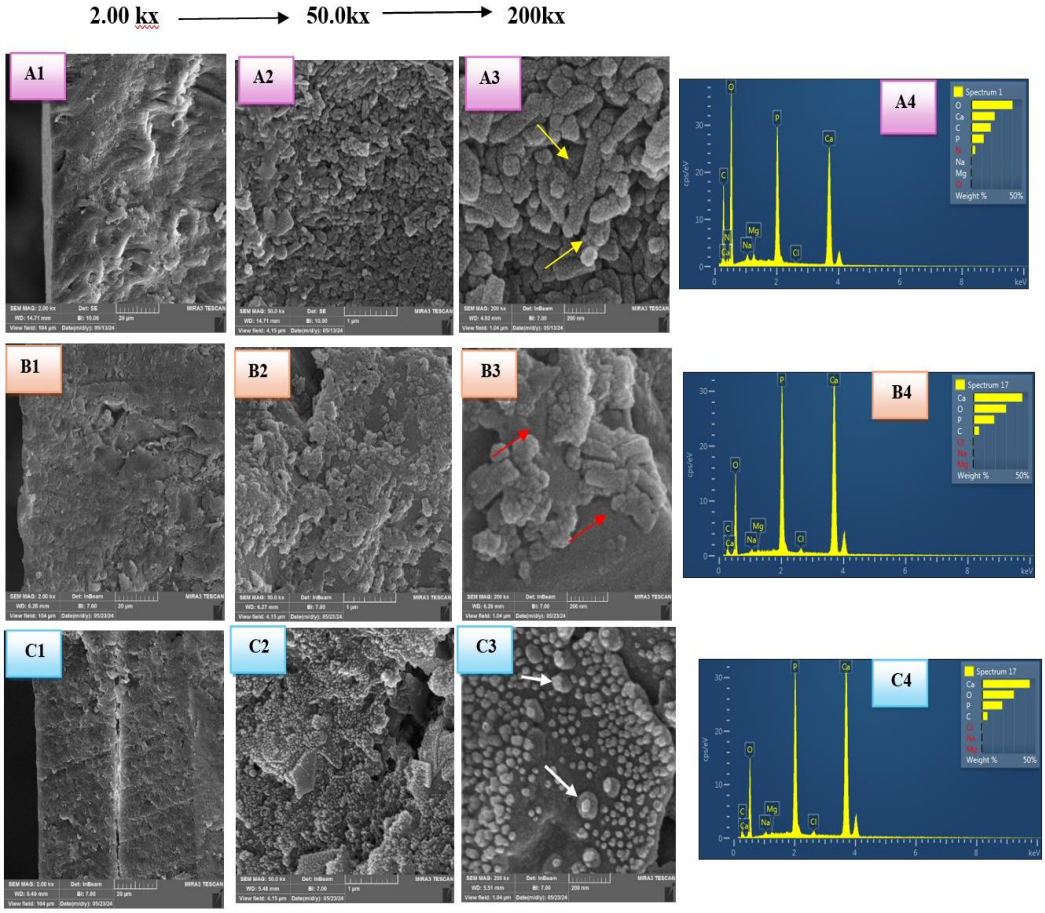

Fig. 7. FESEM images of the teeth cross section after remineralization at different magnifications: A1, A2, A3 for control group; Yellow arow showed the inter-rods spaces. B1, B2, B3 for 5%NCGP, the red arrows showed a decrease in the spaces. C1, C2, C3 for 10%NCGP, the white arrows represent the calcium phosphate precipitation. A4, B4, C4 showed the EDX analysis for each group.

In the EDX analysis (Fig. 7A4, B4, C4), the primary elements detected in enamel were oxygen (O), calcium (Ca), and phosphorus (P), with smaller amounts of carbon (C), magnesium (Mg), sodium (Na), and chloride (Cl).

Table 4 summarizes the means, standard deviations, and Tukey test results for the weight percentages of mineral concentrations. ANOVA revealed significant differences in calcium and phosphate concentrations among the three groups following remineralization ($P < 0.05$). The 5% and 10% NCGP groups had significantly higher mean calcium and phosphate levels than the control group. The 5% NCGP group showed a non-significantly higher mean calcium and phosphate content than the 10% NCGP group.

Comparison of the Ca/P ratio using ANOVA revealed significant differences among the three groups after remineralization ($P < 0.05$). The 5% and 10% NCGP groups exhibited significantly higher mean Ca/P ratios than the control group. The 10% NCGP group showed a non-significantly higher mean Ca/P ratio than the 5% NCGP group (Table 4).

Table 4. Descriptive statistics and multiple comparisons Post-hoc Tukey test of EDX results of calcium wt. %, phosphate wt. % and Ca/P ratio of the control, 5% NCGP, 10% NCGP.

Elements	Control (n=5)	5% NCGP (n=5)	10% NCGP (n=5)	p-value	Tukey test* Control	Tukey test* 5%NCGP	Tukey test* 10%NCGP
Ca wt % (mean±SD)	26.42±6.46	37.48±4.27	34.73±3.69	0.011	A	B	B
P wt % (mean±SD)	13.98±2.18	18.13±1.33	16.77±0.68	0.003	A	B	B
Ca/P (mean±SD)	1.87± 0.18	2.06±0.08	2.06±0.137	0.008	A	B	B

NCGP: Nano-Chitosan/Gallic acid Primer, Ca: Calcium, P: Phosphate, Ca/P: Calcium to Phosphate ratio, SD: Standard deviation, different litters mean significant difference ($P \leq 0.05$).

DISCUSSION

This study aimed to improve orthodontic adhesives' remineralizing, antibacterial, and mechanical properties by modifying them with nano-chitosan loaded with gallic acid. Since all these properties showed improvement, the null hypothesis was rejected.

Many researchers have considered chitosan [32–34] and gallic acid [35,36] potent antibacterial and remineralizing agents. In our study, both materials were combined to achieve a synergistic effect. Moreover, chitosan enables controlled and sustained drug release, which is crucial during the prolonged duration of orthodontic treatment.

Two types of bacteria were investigated: *Streptococcus mutans*, responsible for the initiation of dental caries, and *Lactobacillus acidophilus*, which contributes to the development and progression of caries pathogenesis. *S. mutans*, characterized by acidogenic, aciduric, and cariogenic properties, is present in small amounts or absent in non-carious teeth. *Lactobacilli*, commonly found in saliva, the vestibular mucosa, and on the tooth surface, can increase with the progression of carious lesions [37].

Chitosan exhibits significant antibacterial activity, which is attributed to its ability to adhere to the negatively charged bacterial cell wall, leading to the inhibition of DNA replication and subsequent cell destruction. Another mechanism contributing to its antibacterial properties is its function as an adhesive agent, attaching to toxin-producing organisms and preventing their growth [38].

The results showed that both 5% and 10% NCGP exhibited antibacterial effects against *Streptococcus mutans* and *Lactobacillus acidophilus*, significantly increasing activity at higher concentrations. These findings are consistent with those of Yao et al. [39], who reported that a 20 mg/mL carboxymethyl chitosan (CMC)-modified adhesive system demonstrated antibacterial activity against *Streptococcus mutans*.

Another study by Shoorgashti et al. [40] reported that Ag/ZnO nanoparticles loaded with polycaprolactone/chitosan composites exhibited antibacterial effects against *Staphylococcus aureus* and *Streptococcus mutans* using the inhibition zone method. Almeshal et al. [41] demonstrated that chitosan nanoparticles of different sizes had similar antibacterial effects and reduced *Streptococcus mutans* populations.

Furthermore, Mirhashemi et al. [42] suggested that chitosan-modified orthodontic composite exhibited antibacterial activity against *Streptococcus sanguinis*, *Streptococcus mutans*, and *Lactobacillus acidophilus*.

Regarding the antibacterial action of gallic acid, Elsharkawy et al. [43] reported that adding varying

concentrations of gallic acid to glass ionomer cement resulted in a significant reduction in bacterial turbidity compared to the control group. The antibacterial properties of gallic acid are attributed to its ability to permanently alter bacterial cell membranes, which may lead to changes in cell wall charge, localized rupture, or pore formation, resulting in the leakage of major intracellular components [44].

The findings from FESEM and EDX analyses indicate that both the 5% and 10% NCGP groups can effectively remineralize demineralized enamel, as evidenced by higher calcium, phosphate, and Ca/P ratios precipitated in the area beyond the adhesive layer—a phenomenon not observed in the control group. Our results are consistent with Cheng et al. [45], who concluded that both Galla chinensis extract (GCE) and gallic acid enhance the remineralization of artificially induced early enamel lesions, as demonstrated by transverse microradiography analysis. However, gallic acid primarily facilitated mineral deposition in the superficial layer, whereas GCE promoted mineral precipitation throughout the lesion body. Tang et al. [46] proposed that in the absence of gallic acid, crystals failed to organize properly. At the same time, its presence led to the formation of spherules, with crystal size decreasing as gallic acid concentration increased. These findings suggest that gallic acid influences the morphology and growth of hydroxyapatite (HAP) crystals, which is considered a key mechanism in remineralization. Parisay et al. [47] reported that 0.5% gallic acid varnish exhibited higher remineralization potential in superficial layers than 2.26% fluoride varnish. Based on these studies, we propose that gallic acid acts as a calcium ion carrier, promoting increased calcium deposition on the carious surface, thereby altering the surface crystalline structure and reducing the channels connecting to the lesion body.

Incorporating a bioactive substance into an adhesive requires careful evaluation of bond strength. Excessively high and low shear bond strength (SBS) can negatively affect treatment outcomes. An SBS exceeding 60 MPa may cause enamel fracture during bracket debonding, whereas an SBS below 6–8 MPa may lead to bracket failure and prolonged orthodontic treatment [48].

The current study demonstrated that incorporating nano-chitosan loaded with gallic acid into the orthodontic primer increases shear bond strength (SBS). Specifically, increasing the NCG concentration from 5% to 10% resulted in a significant enhancement of SBS within the acceptable range compared to the control group. These findings support previous studies by Katyal et al. [38] and Mohammed et al. [49], which reported increased mean SBS values following adding chitosan to orthodontic primers.

The increase in SBS observed in NCGP can be attributed to the nanoparticles acting as stress-absorbing elements, providing structural reinforcement and reducing interfacial stress concentration [50].

The adhesive remnant index (ARI) scores for the SBS ranged between 2 and 3. Approximately 53.3% of bond failures occurred at the bracket/adhesive interface, while 36.6% were cohesive failures within the adhesive. This indicates that more than half of the orthodontic adhesive remained on the tooth surface after bracket debonding, consistent with several previous studies [51–53]. An ARI score of 3 is advantageous as it reduces the risk of enamel fracture during debonding [54].

In this study, the degree of conversion (DC) was evaluated to determine the proportion of monomers that react to form polymers, specifically the percentage of C=C double bonds converted into C–C single bonds [55]. The DC significantly influences the physical properties of the resulting cross-linked polymers. A high DC generally correlates with improved mechanical properties, reduced susceptibility to degradation, and lower levels of residual monomers in the organic matrix, leading to decreased monomer leaching and cytotoxic effects [56].

Our study demonstrated that the degree of monomer conversion significantly increased, enhancing adhesive polymerization in the 5% and 10% NCGP groups compared to the control group. These results are consistent with those of Tanaka et al. [57], who reported that adding chitosan loaded with dibasic calcium phosphate fillers increased the DC of dental composites.

In contrast, Mahapoka et al. [58] reported a non-significant decrease in the degree of conversion (DC) when chitosan whiskers were incorporated into dental resin compared to the control group. Similarly, Machado et al. [56] found that adding 2 or 5 wt.% of chitosan or triclosan-loaded chitosan resulted in non-significant differences in DC compared to the control group. This discrepancy may be attributed to the use of solid-form chitosan in both studies, which can hinder light transmission through the adhesive film and slow down the photopolymerization process [59]. In contrast, our study utilized chitosan loaded with gallic acid in liquid form, which did not affect the translucency of the primer nor interfere with

the polymerization process.

All groups' mean degree of conversion (DC) fell within the clinically acceptable range suggested by Kauppi and Combe [60], typically ranging from 55% to 75%. The observed improvement in DC in our study may be attributed to the photooxidative degradation of chitosan during light curing of the modified primer. This degradation leads to the breaking of polymer chains and the generation of free radicals, which reduce the molecular weight and viscosity of the polymer, thereby enhancing the polymerization process and increasing the DC [61, 62].

LIMITATIONS

1. This in vitro study was conducted under controlled laboratory conditions, which may not accurately replicate the complex oral environment.
2. The remineralization assessment was conducted over a fixed period (4 months). Longer-term studies may provide a more comprehensive understanding of the durability and effectiveness of the modified adhesives.
3. Additional studies were required to assess the effectiveness of a broader range of bacteria, including oral biofilm and other cariogenic pathogens.

CONCLUSIONS

Based on the study results, the following conclusions were drawn:

1. The addition of both 5% and 10% nano-chitosan/gallic acid to the orthodontic primer improved the mechanical and chemical properties of the adhesives, including shear bond strength (SBS), adhesive remnant index (ARI), and degree of conversion (DC).
2. Both modified primer groups (5% and 10% NCGP) exhibited antibacterial activity and the capability to remineralize demineralized enamel surfaces.
3. Nano-chitosan/gallic acid is a promising agent for preventing white spot lesions (WSLs) for the following reasons: (i) Chitosan acts as a bio-adhesive between demineralized enamel and the loaded bioactive materials. (ii) Gallic acid serves as a calcium ion carrier, promoting the growth of hydroxyapatite crystals. (iii) Both materials exhibit antibacterial properties against *Streptococcus mutans* and *Lactobacillus acidophilus*.

SUGGESTIONS

Future studies are needed to evaluate the biological properties of chitosan loaded with gallic acid under in vivo conditions. Additionally, further research is required to assess the incorporation of chitosan/gallic acid into other dental products such as toothpaste, varnishes, and other preventive agents.

ACKNOWLEDGEMENT

The authors wish to express their gratitude to the College of Dentistry, University of Mosul, for providing all necessary assistance that helped them to conduct this research.

CONFLICT OF INTEREST

There are no conflicts of interest.

AUTHOR'S CONTRIBUTIONS

Al-Banaa LR: Methodology, Investigation, Resources, Data Curation, Writing – Original Draft Preparation, Writing – Review & Editing, Visualization. Alkhatib AR Supervision. Jabrail FH: Supervision.

FINANCIAL SUPPORT AND SPONSORSHIP

The study was conducted without financial assistance or funding from any agency or organization.

REFERENCES

1. Triwardhani A, Budipramana M, Sjamsudin J. Effect of different white-spot lesion treatment on orthodontic shear strength and enamel morphology: In vitro study. J Int Oral Health. 2020; 12:120-128.
2. Al-Banaa LR, Alsoufy SS, Al-Khatib AR. Factors Contributing to Microleakage in Orthodontics: A Review of Literature. Al-Rafidain Dent J. 2022; 22(2):376–388.
3. Ciribè M, Cirillo E, Mammone M, Vallogini G, Festa P, Piga S, Ferrazzano GF, Galeotti A. Efficacy of F-ACP-Containing Dental Mousse in the Remineralization of White Spot Lesions after Fixed Orthodontic Therapy: A Randomized Clinical Trial. Biomedicines. 2024; 12(6):1202.
4. Shankarappa S, Burk JT, Subbaiah P, Rao RN, Doddawad VG. White spot lesions in fixed orthodontic treatment: Etiology, pathophysiology, diagnosis, treatment, and future research perspectives. J Orthod Sci. 2024; 13:21.
5. Zhang N, Chen C, Weir MD, Bai Y, Xu HH. Antibacterial and protein-repellent orthodontic cement to combat biofilms and white spot lesions. J Dent. 2015;43(12):1529-1538.
6. Chambers C, Stewart S, Su B, Sandy J, Ireland A. Prevention and treatment of demineralization during fixed appliance therapy: a review of current methods and future applications. BDJ. 2013; 215(10):505-511.
7. Alsoufy SS, Al-Banaa LR, Al-Khatib AR, Natural Products Applications in Orthodontics: A Review, Al-Rafidain Dent J. 24 (2024) 499–508.

8. Wang LF, Luo F, Xue CR, Deng M, Chen C, & Wu H. Antibacterial effect and shear bond strength of an orthodontic adhesive cement containing Galla chinensis extract. Biomed Rep. 2016; 4(4): 507-511.
9. Alkasso IR, Al Qassar SS, Taqa GA. Durability of different types of Mouthwashes on the Salivary Buffering system in Orthodontic Patients. Dentistry 3000. 2021;9(1):178-92.
10. Gao, S. S., Qian, L. M., Huang, S. B., & Yu, H. Y. Effect of gallic acid on the wear behavior of early carious enamel. Biomed Mater. 2009; 4(3): 034101.
11. Liu Z, Liu T, Li J, Zhou X, Zhang J. The effect of Galla chinensis on the demineralization of enamel. Journal of Sichuan University. Med Sci. 2003; 34(3):507-509.
12. Chu J P, Li J Y, Hao Y Q and Zhou X D. Effect of compounds of Galla chinensis on remineralization of initial enamel carious lesions in vitro. J Dent. 2007; 35: 383–387.
13. Nader AH, Sodagar A, Akhavan A, Pourhajibagher M, Bahador A. Antibacterial effects of orthodontic primer harboring chitosan nanoparticles against the multispecies biofilm of cariogenic bacteria in a rat model. Folia Med (Plovdiv). 2020; 62(4):817-824.
14. Husain, S., Al-Samadani, K. H., Najeeb, S., Zafar, M. S., Khurshid, Z., Zohaib, S., & Qasim, S. B. Chitosan biomaterials for current and potential dental applications. Materials. 2017; 10(6): 602.
15. Simeonov, M., Gussiyska, A., Mironova, J., Nikolova, D., Apostolov, A., Sezanova, K., & Vassileva, E. Novel hybrid chitosan/calcium phosphates microgels for remineralization of demineralized enamel–a model study. Eur. Polym. J. 2019; 119:14-21.
16. Nimbeni, S. B., Nimbeni, B. S., & Divakar, D. D. Role of Chitosan in Remineralization of Enamel and Dentin: A Systematic Review. Int J Clin Pediatr Dent.. 2021; 14(4), 562.
17. Santoso T, Djauharie NK, Kamizar, et al. Carboxymethyl chitosan/ amorphous calcium phosphate and dentin remineralization. J Int Dent Med Res. 2019; 129(1):84–87.
18. Soran, Z.; Aydin, R.S.; Gumusderelioglu, M. Chitosan scaffolds with BMP-6 loaded alginate microspheres for periodontal tissue engineering. J Microencapsul. 2012; 29: 770–780.
19. Hameed AR, Majdoub H, Jabrail FH. Effects of Surface Morphology and Type of Cross-Linking of Chitosan-Pectin Microspheres on Their Degree of Swelling and Favipiravir Release Behavior. Polymers. 2023;15(15):3173.
20. Esmaeili M, Rajabi L, Bakhtiari O. Preparation and characterization of chitosan-boehmite nanocomposite membranes for pervaporative ethanol dehydration. J Macromol Sci, Part A. 2019; 56(11):1022-1034.
21. Saxena K, Ann CM, Azwar MA, Banavar SR, Matinlinna J, Peters OA, Daood U. Effect of strontium fluoride on mechanical and remineralization properties of enamel: An in-vitro study on a modified orthodontic adhesive. Dent Mater. 2024; 40(5):811-823.
22. Gutiérrez MF, Malaquias P, Matos TP, Szesz A, Souza S, Bermudez J, Reis A, Loguercio AD, Farago PV. Mechanical and microbiological properties and drug release modeling of an etch-and-rinse adhesive containing copper nanoparticles. Dent Mater. 2017;33(3):309-320.
23. Alkhayat, Z.I., Salih Al Qassar, S.S., Qasim, A.A. The effect of the static magnetic field on some of the mechanical properties of glass ionomer cement. Ro J Stomato. 2023, 69(4): 227–233
24. Al-Banaa LR. Evaluation of microleakage for three types of light cure orthodontic band cement. J Oral Biol Craniofac Res. 2022;12(3):352-357.
25. Musleh RT, Al-Khatib AR. Effects of Modifying Orthodontic Adhesive by Thymus Vulgaris Essential Oil on Shear Bond Strength of the Brackets. J Surv Fish Sci. 2023;10(3S):3510-3519.
26. Abdulhaddi A, Al Qassar SS, Mohammed AM. Assessment of the mechanical properties and antimicrobial efficiency of orthodontic adhesive modified with Salvadora Persica oil. Ro J Stomatol. 2024;70(2):153-159.
27. EL-Awady AA, Al-Khalifa HN, Mohamed RE, Ali MM, Abdallah KF, Hosny MM, Mohamed AA, ElHabbak KS, Hussein FA. Shear bond strength and antibacterial efficacy of cinnamon and titanium dioxide nanoparticles incorporated experimental orthodontic adhesive—an in vitro comparative study. Appl. Sci. 2023;13(10):6294.
28. Al Taweel SM, Zinelis S, Sofyan A, Al Jabbari YS. Does surface priming increase the bond strength of orthodontic brackets? An experimental study. Clin Exp Dent Res. 2024;10(3): e888.
29. Mohammed MH, Hasan BA. Equisetum ramosissimum desf-assisted green synthesis of cerium oxide nanoparticles: Characterization and antimicrobial potential against cariogenic Streptococcus mutans. Nanomed J. 2024; 11(3): 250-267.
30. Gouvêa DB, Santos NM, Pessan JP, Jardim JJ, Rodrigues JA. Enamel subsurface caries-like lesions induced in human teeth by different solutions: a TMR analysis. Braz Dent J. 2020;31(2):157-163.
31. Taqa AA, Sulieman RT. artificial saliva sorption for three different types of Dental composite resin An in vitro study. Al-Rafidain Dent J. 2011;11(3):296-302.
32. Valian A, Goudarzi H, Nasiri MJ, Roshanaei A, Sadeghi Mahounak F. Antibacterial and Anti-biofilm Effects of Chitosan Nanoparticles on Streptococcus Mutans Isolates. J Iran Med Counc. 2023;6(2):292-298
33. Garcia LG, ROCHA MG, Freire RS, Nunes PI, Nunes JV, Fernandes MR, Pereira-Neto WA, Sidrim JJ, Santos FA, Rocha MF, Rodrigues LK. Chitosan microparticles loaded with essential oils inhibit duo-biofilms of Candida albicans and Streptococcus mutans. J Applied Oral Sci. 2023; 31:e20230146.
34. Rajabnia R, Ghasempour M, Gharekhani S, Gholamhoseinnia S, Soroorhomayoon S. Anti-Streptococcus mutans property of a chitosan: Containing resin sealant. J Int Soc Prevent Communit Dent. 2016; 6:49-53.
35. Passos MR, Almeida RS, Lima BO, de Souza Rodrigues JZ, de Macêdo Neres NS, Pita LS, Marinho PD, Santos

IA, da Silva JP, Oliveira MC, Oliveira MA. Anticariogenic activities of Libidibia ferrea, gallic acid and ethyl gallate against Streptococcus mutans in biofilm model. J Ethnopharmacol. 2021; 274:114059.
36. Goyal D, Rather SA, Sharma SC, Mahmood A. In vitro anticariogenic effect of gallic acid against Streptococcus mutans. Indian J Exp Biol. 2022; 58(07):445-451.
37. Ünal S, Bakir SE, Bakir EP. Evaluation of the Antibacterial Effects of Four Different Adhesives Against Three Bacterial Species in Two Time Periods: An In Vitro Comparative Study. J Adv Oral Res. 2022; 13(1):120-126.
38. Katyal D, Jain RK, Sankar GP, Prasad AS. Antibacterial, cytotoxic, and mechanical characteristics of a novel chitosan-modified orthodontic primer: An in-vitro study. J Int Oral Health. 2023; 15:284-289.
39. Yao S y, Chen SP, Wang RX, Zhang K, Lin XX, Mai S. Antibacterial activity and bonding performance of carboxymethyl chitosan–containing dental adhesive system. Int J Adhes. 2022; 119:103269.
40. Shoorgashti R, Havakhah Sh, Nowroozi S, Ghadamgahi B, Mehrara R, Oroojalian F. Evaluation of the antibacterial and cytotoxic activities of Ag/ZnO nanoparticles loaded polycaprolactone/chitosan composites for dental applications. Nanomed J. 2023; 10(1): 68-76.
41. Almeshal R, Pagni S, Ali A, Zoukhri D. Antibacterial Activity and Shear Bond Strength of Orthodontic Adhesive Containing Various Sizes of Chitosan Nanoparticles: An In Vitro Study. Cureus. 2024; 16(2): e54098.
42. Mirhashemi AH, Bahador A, Kassaee MZ, Daryakenari GH, Ahmad Akhondi MS, Sodagar A. Antimicrobial Effect of Nano-Zinc Oxide and Nano-Chitosan Particles in Dental Composite Used in Orthodontics. J Med Bacteriol. 2013; 2 (3, 4): 1-10.
43. Elsharkawy SM, Gomaa YF, Gamal R. Experimental Glass Ionomer Cement Containing Gallic acid: Antibacterial Effect and Fluoride Release an in vitro Study. Open Access Macedonian J Med Sci. 2022; 25;10(D):131-6.
44. Borges A, Ferreira C, Saavedra MJ, Simoes M. Antibacterial activity and mode of action of ferulic and gallic acids against pathogenic bacteria. Microb Drug Resist. 2013;19(4):256-65.
45. Cheng L, Li J, Hao Y, Zhou X. Effect of compounds of Galla chinensis and their combined effects with fluoride on remineralization of initial enamel lesion in vitro. J Dent. 2008; 36(5):369-373.
46. Tang B, Yuan H, Cheng L, Zhou X, Huang X, Li J. Control of hydroxyapatite crystal growth by gallic acid. Dent Mater J. 2015; 34(1):108-113.
47. Parisay I, Boskabady M, Bagheri H, Babazadeh S, Hoseinzadeh M, Esmaeilzadeh F. Investigating the efficacy of a varnish containing gallic acid on remineralization of enamel lesions: an in vitro study. BMC Oral Health. 2024; 24(1):175.
48. Pourhajibagher M, Sodagar A, Bahador A. An in vitro evaluation of the effects of nanoparticles on shear bond strength and antimicrobial properties of orthodontic adhesives: A systematic review and meta-analysis study. Int Orthod. 2020; 18(2):203-13.
49. Mohammed, R. R., & Rafeeq, R. A. Evaluation of the shear bond strength of chitosan nanoparticles-containing orthodontic primer: An in vitro study. International J Dent. 2023(1): 9246297.
50. Al-Banaa, L. R., Al-Khatib, A., & Jabrail, F. H. (2024). The Antibacterial and remineralizing effects of orthodontic adhesive modified by nano-chitosan loaded with calcium phosphate. Braz Dent Sci. 2024; 27(4):e4552.
51. Ahmed T, Rahman NA, Alam MK. Comparison of orthodontic bracket debonding force and bracket failure pattern on different teeth in vivo by a prototype debonding device. Biomed Res Int. 2021; 2021(1):6663683.
52. Santos LK, Rocha HR, Pereira Barroso AC, Otoni RP, de Oliveira Santos CC, Fonseca-Silva T. Comparative analysis of adhesive remnant index of orthodontic adhesive systems. South Eur J Orthod Dentofac Res. 2021; 8(2):26-30.
53. Sharma P, Jain AK, Ansari A, Adil M. Effects of different adhesion promoters and deproteinizing agents on the shear bond strength of orthodontic brackets: An: in vitro: study. J Orthod Sci. 2020; 9(1):2.
54. Northrup RG, Berzins DW, Bradley TG, Schuckit W. Shear bond strength comparison between two orthodontic adhesives and self-ligating and conventional brackets. Angle Orthod 2007; 77(4):701-706.
55. Xu T, Li X, Wang H, Zheng G, Yu G, Wang H, et al. Polymerization shrinkage kinetics and degree of conversion of resin composites. J Oral Sci. 2020; 62(3):275-280.
56. Machado AH, Garcia IM, da Motta AD, Leitune VC, Collares FM. Triclosan-loaded chitosan as antibacterial agent for adhesive resin. J Dent. 2019; 83:33-39.
57. Tanaka CB, Lopes DP, Kikuchi LN, Moreira MS, Catalani LH, Braga RR, Kruzic JJ, Gonçalves F. Development of novel dental restorative composites with dibasic calcium phosphate loaded chitosan fillers. Dent Mater. 2020; 36(4):551-559.
58. Mahapoka E, Arirachakaran P, Watthanaphanit A, Rujiravanit R, Poolthong S. Chitosan whiskers from shrimp shells incorporated into dimethacrylate-based dental resin sealant. Dent Mater J. 2012;31(2):273-279.
59. Altmann, A.S.P., Collares, F.M., Balbinot, G.S., Leitune, V.C.B., Takimi, A.S., Samuel, S.M.W. Niobium pentoxide phosphate invert glass as a mineralizing agent in an experimental orthodontic adhesive. Angle Orthod. 2017; 87 (5), 759–765.
60. Kauppi, M.R., Combe, E.C. Polymerization of orthodontic adhesives using modern high-intensity visible curing lights. Am J Orthod Dentofacial Orthop. 2003; 124 (3): 316–322.
61. Sionkowska A, Płanecka A, Lewandowska K, Kaczmarek B, Szarszewska P. Influence of UV-

irradiation on molecular weight of chitosan. Prog Chem Appl Chitin Deriv. 2013;18(18):21-28.
62. Al-Banaa, LR., Al-Khatib, AR., & Jabrail, FH. Evaluation of the biological, physical, mechanical and chemical properties of orthodontic primer modified by nano-chitosan loaded with bioactive materials. J Oral Biol Craniofac Res. 2025; 15(3): 500-507.